Measurement of magnetic hysteresis loops of the Ni-5at.%W alloy substrate as a function of temperature in a stack of 2G HTS coated conductor annuli

Sébastien Brialmont, Jean-François Fagnard, Benoît Vanderheyden, Frédéric Mazaleyrat, Seungyong Hahn, Anup Patel, and Philippe Vanderbemden

Abstract—The development of coated conductors with a ferromagnetic substrate and their use in various applications require an accurate knowledge of the magnetic properties of the substrate. In this work, we report measurements in AC regime (30 Hz) of the magnetic hysteresis loops of the Ni-5at.%W alloy ferromagnetic substrate in a stack of 2G YBCO tapes cut in the shape of annuli from 46 mm wide coated conductors. The stacked annuli form a closed magnetic circuit which is the ideal configuration due to the absence of demagnetizing effect. The measurements are carried out at four temperatures between 77 K and 293 K. The peak intensity of the relative permeability is not significantly affected in the range of temperature considered. The coercive field dependence with temperature is also investigated. The hysteresis losses Q as a function of the amplitude of the flux density B_{m} exhibit a power law behavior ($Q \sim B_{\mathrm{m}}^n$) at the four temperatures. This power law behavior is also studied at low fields under the presence of a DC bias field. Finally, the hysteresis loops can be reproduced with the Jiles-Atherton model, which is used to estimate the hysteresis parameters and to discuss their temperature dependence.

Index Terms—Coated conductors, Ni-5at.%W substrate, magnetic properties measurement, magnetic hysteresis, high-temperature superconductors (HTS).

I. Introduction

SECOND generation (2G) coated conductors have been widely used in engineering applications: field trapping [1], magnetic shielding [2] or large scale power applications including SMES (Superconducting Magnetic Energy Storage), superconducting power cables and superconducting transformers [3]. Beside, coated conductors are also used in medical applications like MRI machines or medical accelerators which require a proper field uniformity. The so-called Rolling Assisted Biaxially Textured Substrates (RABiTS) process provides an excellent template for depositing High Temperature Superconductors (HTS) [4]. This technique and the ability to produce highly textured buffer layers are fundamental to produce low cost superconducting tapes with a good uniformity, mechanical robustness and electrical stability over long length. Over last years, these coated conductors have been shown to carry large current densities ($> 10^6$ A/cm^2) under the presence of magnetic fields and at temperature down to 77 K. RABiTS are typically made of Ni-W alloys which are slightly ferromagnetic [5], [6]. Details about interactions between

the ferromagnetic substrate and the superconducting layer are not fully elucidated today and remain an active research topic. Nevertheless, it is well known that the ferromagnetic substrate can influence the transport critical current in coated conductors [7]. In several situations, the presence of a magnetic substrate brings undesired effects since it affects the AC losses in the coated conductors, either due to a modification of the magnetic field in the tapes or directly due to magnetic hysteresis losses [8]–[15]. Such effects have consequences on the properties of coated conductors involved in applications such that power cables [16], [17] or pancake coils [18], [19] and should be included in the modelling [20], [21]. There are nevertheless situations where the presence of a magnetic material close to the superconductor may bring improvements of a superconducting system. This is the case for low frequency passive magnetic shielding, for which two advantages can be noticed. Due to its ability to channel magnetic flux lines, a ferromagnetic substrate may improve the shielding process itself, similarly to the impact of combining bulk ferromagnetic and superconducting shields [22]–[26]. The second advantage is that a non-zero magnetic shielding persists above T_c [27], thereby increasing the reliability of the shield.

Accordingly, an accurate knowledge of the substrate magnetic properties is crucial to assess its influence on the performances of the applications involving coated conductors. Most of the existing methods are based on inductive techniques using a magnetizing coil to magnetize the sample and a pick-up B-coil to measure the magnetic flux density. In order to magnetize the sample uniformly up to high value of magnetic flux density, the measurement methods should ideally consist of a closed magnetic circuit. In order to be able to determine the magnetic field H directly from Ampere's law, the best configurations are specimens already in the shape of a closed magnetic circuit like toroidal or ring samples [28]. If such a configuration cannot be achieved, it is sometimes better to measure the tangential component of the H field, as described by Tumanski [28]. As the tangential component of H is conserved at the interface of two different materials, an external H-coil can be used to measure the H field inside the sample [29] provided the coil is perfectly tangential to the sample. This technique

can also be improved by using two H-coils, based on the assumption that the H field evolves linearly in the air layer close to the sample [30]. Measurement techniques involving magnetometers e.g. Superconducting QUantum Interference Devices (SQUID) [31], [32] or an extraction magnetometer [33] are sometimes used. However, such magnetometers do not accommodate sizeable samples (i.e. more than a few mm in length). Moreover, H inside the material is generally quite different from the applied field H_{ext}. SQUID can also be used for loss measurements but at frequencies much lower than in practical applications [34]. Finally, Claassen *et al.* use an inductive method applied on straight magnetic ribbons; although the *B-H* curves are affected by demagnetization effects, this technique is appropriate for determining their coercive field, saturation field, and AC losses [35].

Very few studies report measurements of magnetic properties of ferromagnetic substrates in coated conductors at the operating temperature of 77 K (liquid nitrogen temperature). Claassen and Thieme [34] report measurements of $B(H)$ data for different Ni-5at.% W RABiTS or composite substrates. The samples are typically $\sim$ 10 cm long tapes characterized using an AC susceptibility measurement apparatus [35] to record $B(H)$ loops at 77 K for AC fields up to $\sim$ 1000 A/m; the results are compared to those obtained by a SQUID. Miyagi *et al.* [36] report magnetic relative permeability measurement results on two kinds of Ni based HTS substrates (strongly and weakly magnetic) as well as their AC losses, both at room and liquid nitrogen temperatures. An empiric law fitting the corresponding experimental permeability and AC loss data vs. the applied field was determined by Nguyen *et al.* [37]. Although this set of available experimental data is extremely valuable, there is no information about how the *B-H* loops evolve between room and liquid nitrogen temperatures. It is also observed that the values of the data obtained independently on the magnetic substrates sometimes need to be modified in order to reconcile the calculated and experimental AC losses [9].

In this paper, the measurements of magnetic properties of a ferromagnetic Ni-5at.% W substrate are carried out on a stack of large width (46 mm) 2G YBCO coated conductors cut in the shape of annuli. Accordingly, the stacked annuli naturally form a closed magnetic circuit which is the ideal configuration as measurements are not affected by the demagnetizing factor. Ferromagnetic hysteresis cycles are measured in low frequency AC regime. Knowing that the possible benefit of the ferromagnetic substrate is also present above T_c, the properties are determined not only at 77 K and room temperature (293 K) but also at two intermediate temperatures (195 K and 238 K). Hysteresis losses as well as the relative permeability are then computed. The results are compared with the Jiles-Atherton model [38] at the different temperatures. Finally, minor hysteresis loops are investigated.

II. EXPERIMENTAL SET-UP

The coated conductors are 46 mm width YBa$_2$Cu$_3$O$_{7-d}$ coated conductors from American Superconductor [39].
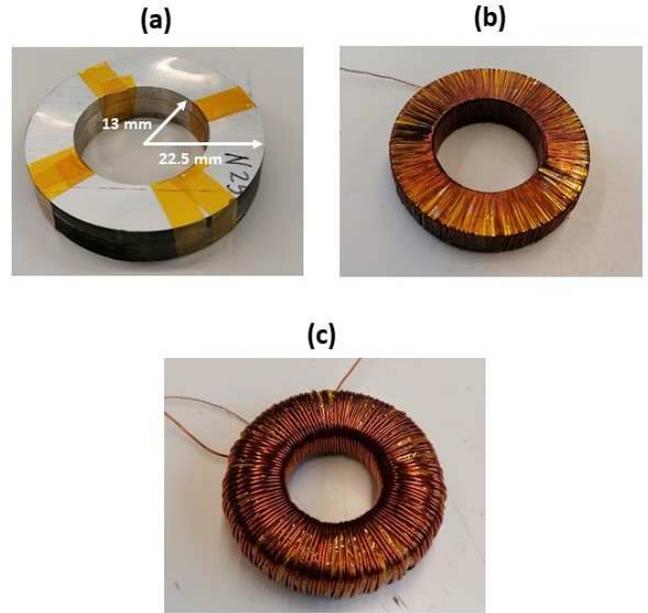

Fig. 1. Pictures of (a) the annular stack of coated conductors with Ni-5at.%W substrate, (b) the secondary winding made with 0.15 mm diameter wire dedicated to the EMF measurement and (c) the primary winding made with 0.6 mm diameter wire devoted to inject the current.

The HTS tapes are based on a Ni-5at.%W RABiTS with a thickness of 75 μm followed by buffer layers deposited by reactive sputtering [40]. The superconducting layer is then deposited using a metal organic deposition process of trifluoroacetate (TFA) based precursors. Its thickness is approximately 1 μm. It is characterized by a nominal critical current by unit width ranging between 200-350 A cm^{-1} at self-field and 77 K. Finally, the stabilizer consists of a 3 μm-thick silver layer. Annuli (outer diameter 45 mm, inner diameter 26 mm) were previously cut from the original coated conductor using spark erosion machining [40]. Several annuli are stacked over a height of 9.8 mm so that they are in the shape of a closed magnetic circuit. The advantages are the absence of demagnetizing field so that we can access to the true $B(H)$ dependence and the convenience to magnetize the sample uniformly up to rather high flux density values by simply winding a magnetizing coil around it. The resulting magnetic circuit has a toroidal shape with a nearly square cross section [28], [35] and is shown in Fig. 1(a).

The measurement method consists of two windings: the primary winding made of 0.6 mm diameter wire in order to inject a current up to 0.6 A, is devoted to the generation of the applied magnetic field H. The magnetic field strength H can be found from the injected current I and the number of turns in the magnetizing coil n_p through

$$H = \frac{n_p I}{l}, \tag{1}$$

where l is the mean magnetic path which can be determined

in a good approximation by:

$$l = 2\pi \frac{R_{\text{out}} - R_{\text{in}}}{\ln(R_{\text{out}}/R_{\text{in}})}, \quad (2)$$

with $1.1 < R_{\text{out}}/R_{\text{in}} < 1.6$ to ensure a sufficient magnetic field uniformity within the sample [28]. In the present configuration, possible differences in the magnetic response may arise depending on whether the magnetizing field direction is parallel to the long side of the tape or parallel to its width. Nevertheless, these differences are fully averaged since the field is applied along the circumference of annuli cut from the tape. Hence, for the analysis of the results, the magnetic properties of the ferromagnetic substrate are then assumed to be isotropic. The secondary winding is devoted to the electro-motive force (EMF) measurement. It is made of one layer of 0.15 mm diameter wire to maximize the number of turns (433 in this case) directly wound on the sample to minimize the influence of the stray field. The magnetic flux density B is then obtained by time integration.

Both the secondary and primary windings are shown in Fig. 1(b) and Fig. 1(c) respectively. As reported in Tumanski's comprehensive handbook [28], a parasitic effect may arise from how the primary is wound due to the fact that, in practice, the windings are slightly slanted with respect to the torus cross section and may generate a spurious magnetic field along the torus axis of revolution. Therefore, if no precaution is taken, a coil uniformly wound is equivalent to a hypothetical single turn located at the mean circumference. This turn may be coupled to a hypothetical single turn formed by the secondary winding. In order to reduce this effect, the primary winding is made of an even number of layers wound along the ring circumference following alternatively the clockwise and anticlockwise way. With such pairs of layers, the turns are slightly slanted in such a way that the contributions of two neighboring layers to the field component along the axis of revolution are expected to cancel out each other. The magnetizing current I is obtained by measuring the voltage across a weakly inductive 16 Ω resistor connected in series with the primary winding. The EMF is measured directly across the secondary winding. Both the current and EMF signals are recorded using a Tektronix TBS 2000B digital oscilloscope. In practice, the injected current I as well as the applied magnetic field H are both sinusoidal. The magnetic circuit and coils are either placed at room temperature (293 K) or cooled, either by a commercial freezer (238 K), dry ice (solid CO_2) pellets (195 K) or liquid nitrogen (77 K). The temperatures are measured with a type K thermocouple connected to a FLUKE 87V multimeter. The applied magnetic field being always parallel to the tapes, it is assumed that the 1-2 μm thick superconducting layers do not contribute to the measured magnetic properties, even under T_c (77 K).

III. RESULTS AND DISCUSSION

A. Hysteresis curves at several temperatures

We first describe major $B(H)$ hysteresis curves, from which the magnetic permeability or the hysteresis losses can be
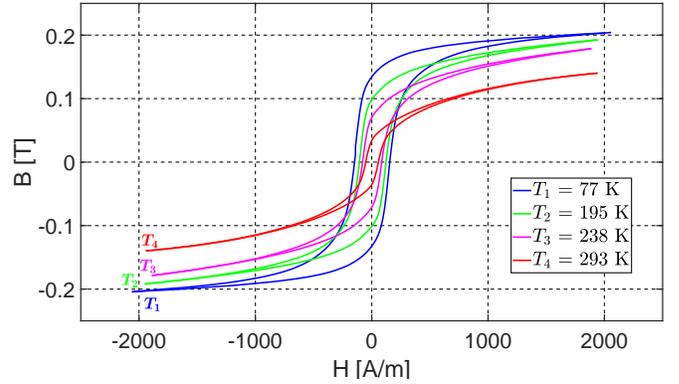
Fig. 2. Hysteresis magnetic cycles recorded at four temperatures on the Ni-5at.%W substrate. The data are obtained at a frequency of 30 Hz.

deduced. The $B(H)$ hysteresis loops at 4 different temperatures (293 K, 238 K, 195 K and 77 K) are compared in Fig. 2. The frequency of AC magnetic field is 30 Hz. When varying the frequency of the applied magnetic field between 20 Hz and 200 Hz, no perceptible difference between the hysteresis curves is found. From the results plotted in Fig. 2, it can be seen readily that the average width of the hysteresis cycle and the saturation magnetization both increase with decreasing temperature. Moreover the reversible region of the curve (i.e. the overlap between ascending and descending branches) is reached at higher magnetic flux densities for lower temperatures. These phenomena are due to the variation of the magnetocrystalline anisotropy with temperature. When the temperature is close to the Curie temperature (339 K and 330 K, as reported in the literature for Ni-5at.%W alloy [31], [41]), the magnetic properties are dominated by the thermal agitation and the behavior is mainly anhysteretic. As the temperature decreases, the behavior is mainly dominated by the anisotropy and the coercive field as well as the remnant magnetization increase.

B. Magnetic permeability

Next, we investigate the effect of the field amplitude on the hysteresis curves. Several magnetizing fields $H = H_{\text{m}}\sin(\omega t)$ of increasing amplitude H_{m} are applied and the amplitude of the magnetic flux density B_{m} is recorded for each amplitude H_{m}. Fig. 3 shows this $B_{\text{m}}(H_{\text{m}})$ dependence at different temperatures as well as the successive applied cycles at 77 K in the inset. From a classic analysis of ferromagnetic materials [42], the $B_{\text{m}}(H_{\text{m}})$ curves give equivalent results to the first magnetization curves. The relative magnetic permeability can be defined as follows:

$$\mu_r = \frac{B_{\text{m}}}{\mu_0 H_{\text{m}}} \quad (3)$$

with μ_0 the magnetic permeability of vacuum.

The effect of temperature on the relative permeability is shown in Fig. 4. Several observations can be made. The first is that all $\mu_r(B_{\text{m}})$ curves display a non-monotonic behavior, with a maximum shifted continuously toward higher magnetic flux densities B_{m} as the temperature decreases from 293 K to 77
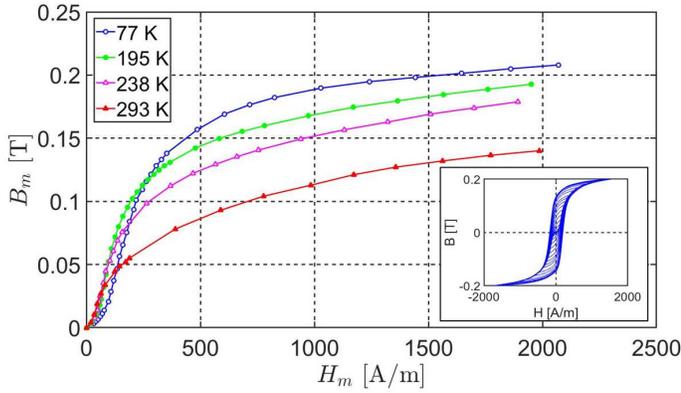
Fig. 3. Peak magnetic flux density B_{m} as a function of the maximal applied magnetic field H_{m} at different temperatures. Several cycles with increasing H_{m} are applied to the sample as shown in the inset for $T = 77$ K.
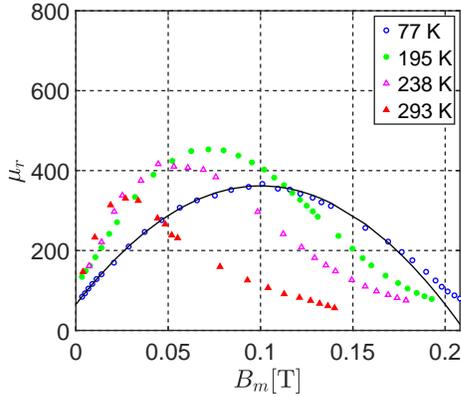

Fig. 4. Relative magnetic permeability as a function of the maximal magnetic flux density at 4 different temperatures. The solid line is the quadratic fitting given by Eq. (4).

K. Second, the temperature does not have a major effect on the peak intensity of the relative permeability, which is found to lie in the range 330 - 440. The measured maximum permeability at 293 K is $\mu_{r,\mathrm{max}} = 330$ at $B_{\mathrm{max}} = 30$ mT and 362 for $B_{\mathrm{max}} = 100$ mT at 77 K. These results are different from those obtained by Miyagi *et al.* [36] on a weakly magnetic substrate: although the B_{max} are the same as in the present study, the values of the peak relative permeability are different ($\mu_{r,\mathrm{max}} \approx 700$ at room temperature, and $\mu_{r,\mathrm{max}} \approx 212$ at 77 K). At liquid nitrogen temperature, our results nicely agree with those found by Claassen *et al.* [9], [34] who found $\mu_{r,\mathrm{max}} = 380$ on the same material. As can be seen in Fig. 4, the initial permeability $\mu_{r,i}$ (obtained by linear extrapolation down to $B_{\mathrm{m}} = 0$ T) lies around $\mu_{r,i} \approx 120$ for the three highest temperatures (293 K, 238 K, 195 K) and is equal to $\mu_{r,i} \approx 70$ at 77 K. The latter value is about 1.5 times the one ($\mu_r \approx 46$) obtained by Miyagi *et al.* [36] and similar to that found by Claassen *et al.* ($\mu_r \approx 65$) [9], [34]. Moreover, the permeability curves measured at 195 K and above exhibit a typical asymmetric shape which has already been highlighted on different ferromagnetic materials when approaching the

Curie temperature [43]. The $\mu_r(B_{\mathrm{m}})$ data at 77 K are almost symmetric on both sides of the maximum. Remarkably, it is found that in the investigated field range, the experimental points obtained at 77 K can be fitted with a simple parabolic law, i.e.

$$\mu_r(B_{\mathrm{m}}) = \mu_{r,i} + (\mu_{r,i} - \mu_{r,\mathrm{max}}) \left[\left(\frac{B_{\mathrm{m}}}{B_{\mathrm{max}}} \right)^2 - 2\frac{B_{\mathrm{m}}}{B_{\mathrm{max}}} \right], \quad (4)$$

as shown by the solid line in Fig. 4, using the fitting parameters: $\mu_{r,i} = 70$, $\mu_{r,\mathrm{max}} = 362$ and $B_{\mathrm{max}} = 100$ mT. Such a $\mu_r(B_{\mathrm{m}})$ dependence as well as the first magnetization curve suggest that the dominating hysteresis mechanism at 77 K is the pinning of domain walls [42]. The results shown in Fig. 3 and Fig. 4, as well as the parabolic law described by Eq. 4, provide useful experimental data which can be incorporated in numerical modelling of structures and applications involving 2G HTS tapes based on Ni-5at.%W RABiTS. Indeed, below the critical temperature, the superconducting properties are dependent on the field distribution inside the HTS layers and thus, their analysis requires an accurate modelling of the ferromagnetic layers themselves. Regarding the data measured at $T > T_{\mathrm{c}}$, the results described above can be used to predict the magnetic reluctance of a structure made of such superconducting tapes that can be used e.g. for magnetic shielding. If the structure is subjected to relatively low magnetic fields (e.g. with $B_{\mathrm{m}} < 0.1$ T), the relatively high values of the magnetic permeability give evidence that a non-zero magnetic shielding effect will persist even if the temperature accidentally rises above the critical temperature of the superconductor.

C. Coercive field

We now turn to the evolution of the coercive field H_{c}, which is also a quantity of definite interest when studying the magnetic properties of a specific material. The temperature has a significant effect on the coercive field as can be seen in Fig. 5.

The panels (a) and (b) show, for each temperature, the coercive field H_{c} expressed either as a function of the amplitude H_{m} of the applied magnetic field or the corresponding amplitude magnetization M_{m} given by

$$M_{\mathrm{m}} = \frac{B_{\mathrm{m}}}{\mu_0} - H_{\mathrm{m}}. \quad (5)$$

Fig. 5(c) shows the temperature dependence of the coercive field H_{c} determined at three field amplitudes $H_{\mathrm{m}} = 50$, 100 and 1500 A/m. At large amplitudes, the coercive field clearly decreases as the temperature increases. The influence of temperature is much less pronounced for low values of magnetizing field. The $H_{\mathrm{c}}(T)$ measured at 1500 A/m displays a quasi-linear behavior. In the crude assumption that H_{c} vs. T remains linear at higher temperatures, an extrapolation shows that H_{c} goes to 0 at $T \approx 420$ K. This value is higher than Curie temperatures for Ni-5at.%W lying between 330 K and 340 K as specified in Section III-A. This suggests that a linear approximation does not hold when approaching the Curie temperature. When plotted as a function of the applied field H_{m} (Fig. 5(a) in log-log scale), the H_{c} data follow roughly a
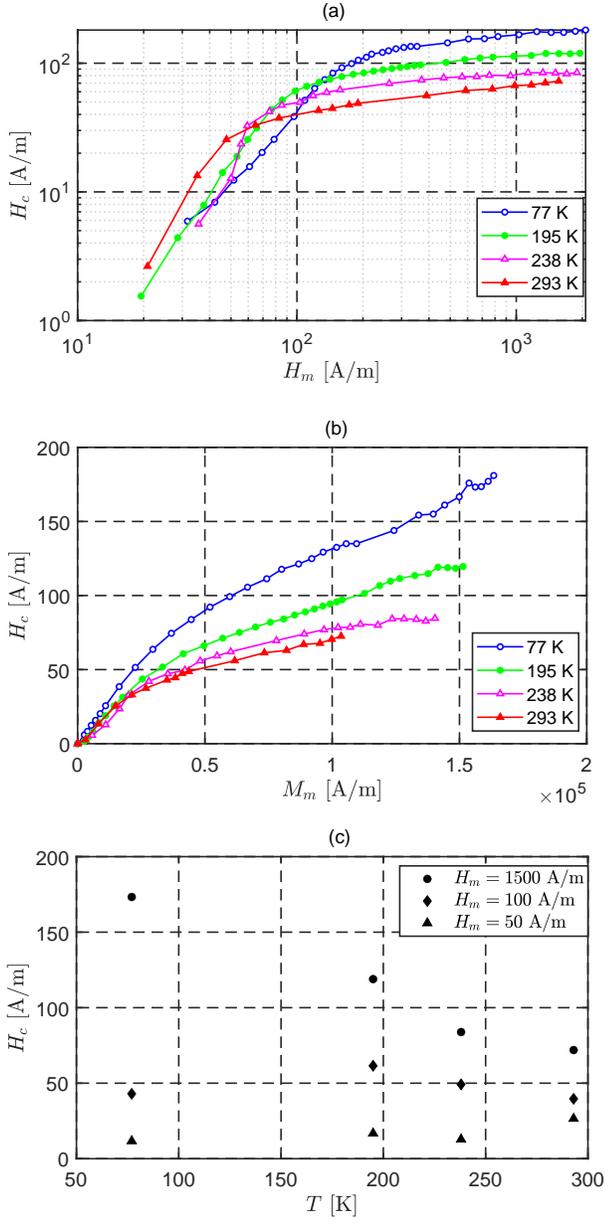
Fig. 5. Evolution of the coercive field H_c as a function of (a) the peak magnetizing field H_m, (b) the peak magnetization M_m, and (c) as a function of temperature.

power law behavior, $H_c \sim (H_m)^n$ at low fields, with n close to 2, followed by a clear kink above which a much weaker field dependence is found. A cross-over of the H_c curves is found between these two regimes, i.e. at low field the highest H_c is found at room temperature (293 K), whereas at high field, the highest H_c occurs at 77 K. It is to be noted that, although a well-defined trend does not clearly emerge, the cross-over found in Fig. 5(a) almost disappears when the coercive field is plotted as a function of the magnetization M_m as shown in Fig. 5(b), leading to the conclusion that for any given value of the magnetization M_m, the highest coercive field is observed at the liquid nitrogen temperature. Finally, let us mention that the amplitude of the coercive field and its temperature dependence

can be used, using interpolation of the data plotted in Fig. 5, to predict the hysteretic behavior of the magnetic substrate at temperatures different from those investigated in the present work and, in particular temperatures ranging between 77 K and the critical temperature of the superconductor.

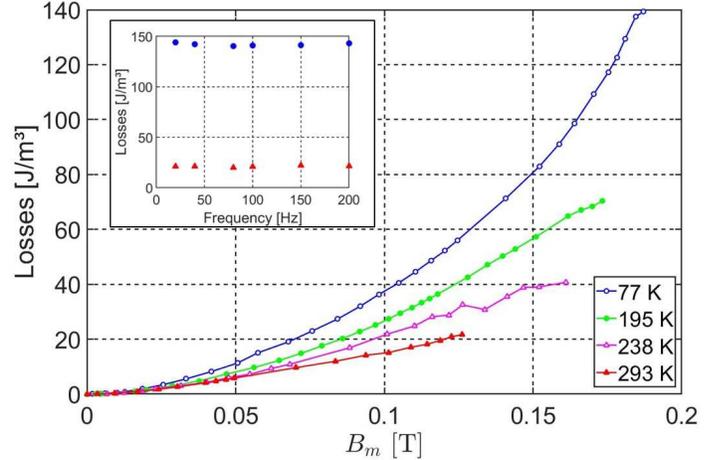### D. Hysteresis losses of major loops

Fig. 6. Hysteresis losses (Q [J/m^3] for one cycle) as a function of the peak magnetic flux density recorded at different temperatures (at a frequency of 30 Hz). In the inset, the losses are plotted as a function of the frequency at 77 K (•) and 293 K (▲) for a fixed H_m of 2000 A/m.

The hysteresis losses in the magnetic substrate are an additional source of losses in HTS coated conductors. In the present configuration, the magnetizing field is applied parallel to the tapes, the superconducting layer is negligible and the only contribution to the losses are those of the magnetic substrate. Depending on the current and the frequency, the hysteresis losses may represent a sizeable fraction of the total AC loss [14]. It is therefore crucial to characterize accurately the hysteresis losses inside the ferromagnetic layers. The evolution of the magnetic losses as a function of the cycle amplitude B_m can be seen in Fig. 6. The losses clearly increase with decreasing temperature. In the present case the frequency has no influence on the measured losses as can be deduced from the inset of Fig. 6 showing the losses (for one cycle) in the frequency range 20 Hz - 200 Hz. Accordingly, the main loss contribution comes from hysteresis losses and not from eddy current losses due to the small thickness of the ferromagnetic substrate ($\approx 75\ \mu$m). Moreover, we can estimate the eddy current contribution to the losses which is given by

$$Q_{\text{eddy}} = \frac{(\pi t B)^2 f}{6\rho},\qquad(6)$$

where t, B and f are respectively the thickness of the substrate, the magnetic flux density and the frequency. The electrical resistivity ρ has been obtained at 77 K and 293 K by a 4-wire sensing method. As can be seen in Table I, the eddy current losses contribution is negligible compared to the hysteresis losses. This result is in agreement with those previously obtained by Miyagi et al. [36] on their weak magnetic

	B [T]	ρ [Ωm]	$\mathbf{Q}_{eddy}$ [J/m^3]
77 K	0.2	2.71 $\times 10^{-7}$	0.041
293 K	0.14	3.6 $\times 10^{-7}$	0.015

substrate. For the 4 temperatures investigated, it can be readily seen that the hysteresis losses follow roughly a power law as a function of the amplitude of B (i.e. $Q \sim Q_0 \left(\frac{B_m}{B_0}\right)^n$), as found experimentally by Miyagi *et. al.* [36], where Q_0 are the losses at the particular flux density $B_m = B_0$. The values of Q_0 and n at the four investigated temperatures can be found in Table II; B_0 is chosen arbitrarily to $B_0 = 0.15$ T to allow for a direct comparison with results from the literature at the liquid nitrogen temperature. Using an empiric fit of the 77 K experimental data, values of $n = 2$ and $n = 1.884$ are found in Gömöry *et al.* [9] and Nguyen *et al.* [37] respectively. The power law behavior is analyzed further in the section below by comparing the losses with or without DC offset.

T [K]	$\mathbf{Q_0}$ [J/m^3]	**n** [-]
77	85.02	2.114
195	55.74	1.779
238	38.77	1.533
293	27.38	1.434

Note that the present geometry, where the magnetizing field is applied parallel to the tapes, corresponds e.g. to the situation arising when the tapes are used to shield a magnetic field parallel to them. The magnetic field configuration here is different from what would be obtained e.g. when the tapes carry an electrical current. If other similar configurations are considered, the obtained intrinsic $B(H)$ data and hysteresis loss data can then be inserted in numerical modelling of the whole structure. In the case where the field is applied perpendicular to the tapes plane, the main contribution to the losses would certainly come from eddy currents which can be computed. Although the field range in our measurements (2000 A/m) is smaller than the field possibly produced by the tapes nominal critical current, the results show that the Ni-W alloy is almost saturated and that magnetizing the sample up to higher field would not drastically change the conclusions. The main change would be to add the (computable) contribution of the eddy current losses.

E. Power law behavior of hysteresis losses

Finally, the application of minor hysteresis loops, i.e. hysteresis loops with a peak magnetization M_m well below the saturation and superimposed to a DC bias field is also investigated in terms of losses. Minor loops can be found in several power engineering applications including rotating machines or

when the superconductor is subjected to ripple voltage from power converters [44]. Moreover, minor hysteresis loops can also be used for the non-destructive detection of structural defects in ferromagnetic materials [45]. Here, we investigate centered hysteresis loops (without any bias DC field) and minor loops with a 500 A/m bias DC field. The evolution of the losses with respect to the peak magnetization M_m is shown in Fig. 7. From this figure, we can directly deduce
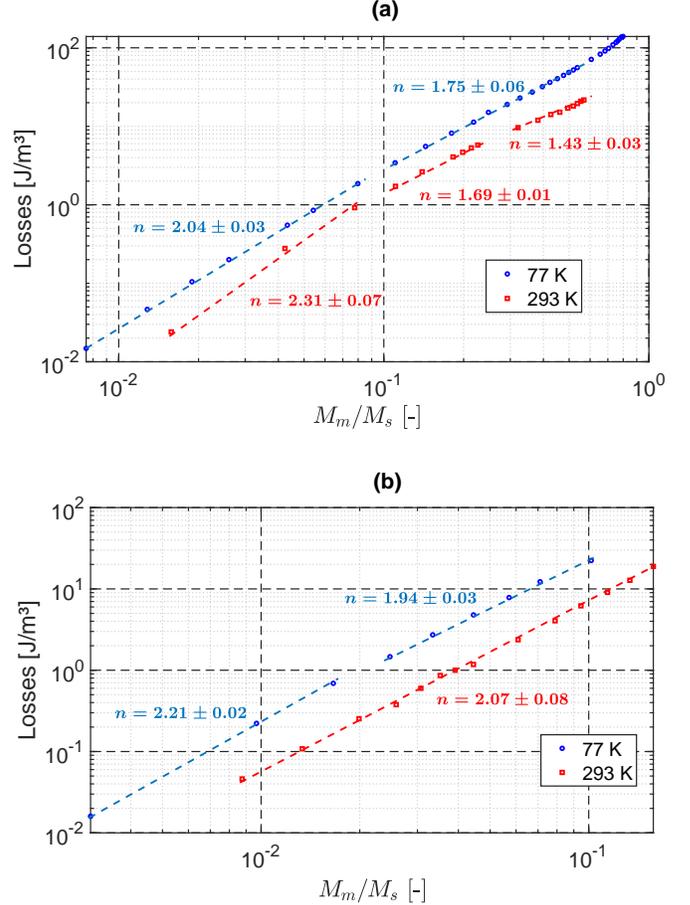

Fig. 7. Evolution of the losses (Q [J/m^3] for one cycle) with the magnetization M_m under the application of minor hysteresis loops. The hysteresis loops are either centered (a) with a bias applied field of 0 A/m or not centered (b) with a bias applied field of 500 A/m. The results are recorded at 293 K and 77 K. The frequency of operation is 30 Hz.

that the hysteresis losses are proportional to $\left(\frac{M_m}{M_s}\right)^n$ with M_s, the saturation magnetization. The method to estimate the saturation magnetization is described in Section III-F. The evolution of the n exponent for several magnetization ranges is also represented in Fig. 7. The general trend is a decreased value of n as the ratio $\frac{M_m}{M_s}$ increases. The losses are always significantly higher at 77 K than at room temperature.

At low fields, the dependence of the losses as a function of the peak magnetization M_m can be partly explained with the Rayleigh model. The model assumes that, for low amplitudes of magnetization, the ascending and descending branches of the hysteresis loop can both be modelled using a quadratic

function. Accordingly, the magnetization can be described by the following equations [46], [47]:

$$M(H) = (\chi_i + bH_m)H \pm \frac{b}{2}\left(H_m^2 - H^2\right), \qquad (7)$$

where χ_i is the initial susceptibility and b is the Rayleigh parameter respectively standing for the reversible part and the irreversible part of the magnetic behavior. From this, the peak magnetization and the hysteresis losses per unit volume for one cycle are respectively given by

$$M_m = M(H_m) = \chi_i H_m + bH_m^2 \qquad (8)$$

and

$$Q = \frac{4}{3}\mu_0 bH_m^3. \qquad (9)$$

From Eq. 8 and Eq. 9, the hysteresis losses are given by

$$Q = \frac{\mu_0}{6b^2}\left(-\chi_i + \sqrt{\chi_i^2 + 4bM_m}\right)^3. \qquad (10)$$

If the behavior is mainly reversible ($b << 1$), Eq. 10 reduces to

$$Q = \frac{4}{3}\mu_0 b\left(\frac{M_m}{\chi_i}\right)^3, \qquad (11)$$

whereas if the irreversible part dominates the magnetic behavior ($b >> 1$), the losses are given by

$$Q = \frac{4}{3}\mu_0 b\left(\frac{M_m}{b}\right)^{3/2}. \qquad (12)$$

As a result, the Rayleigh model predicts a dependence $Q \propto M_m^n$ with n taking a value between 1.5 and 3 depending on the relative importance of the reversible and the irreversible components of the magnetic behavior. In general, the value of n depends on the type of ferromagnetic material, temperature and mechanical stress [46]. For the set of experimental data obtained in the present work, the exponents found are well within the theoretically expected range.

F. Temperature dependence of hysteresis parameters

The dependence on temperature of the magnetic properties of Ni-5at.%W magnetic substrate is rather complex to explain and the experimental results remain difficult to interpret physically. The literature remains indeed very descriptive when relating the effect of temperature on the hysteresis macroscopic magnetic properties. Nevertheless, we choose to discuss the experimental results by fitting them with the phenomenological Jiles-Atherton (J-A) model [38]. In order to find the parameters leading to the best fit of the experimental curves, the procedure is inspired from that described by Pop and Caltun [48].

Basically the J-A model considers the total magnetization M as a sum of an irreversible component M_{irr} and a reversible one M_{rev}: $M = M_{irr} + M_{rev}$. The irreversible component of the magnetization is given by

$$dM_{irr} = \frac{M_{an} - M_{irr}}{k\delta - \alpha(M_{an} - M_{irr})}dH, \qquad (13)$$

Where k and α are two of the J-A model parameters which are described further in this section. In this equation, $\delta = 1$ if $dH/dt > 0$ and $\delta = -1$ if $dH/dt < 0$. The anhysteretic magnetization M_{an} is given by the following Langevin's function:

$$M_{an} = M_s\left(\coth\frac{H_e}{a} - \frac{a}{H_e}\right), \qquad (14)$$

where M_s is the saturation magnetization and a is another parameter within the model. The effective field H_e is defined as

$$H_e = H + \alpha M. \qquad (15)$$

Finally, the reversible magnetization being defined as a fraction c of the difference between the anhysteretic and the irreversible magnetization: $M_{rev} = c(M_{an} - M_{irr})$, the total magnetization is given by

$$M = cM_{an} + (1 - c)M_{irr}. \qquad (16)$$

As a result, in addition to the saturation magnetization, the model includes 4 other fitting parameters c, k, a and α from which modelled hysteresis curves can be found. The comparison between the experimental hysteresis cycles and the fitting curves as well as the corresponding model parameters are shown in Fig. 8 for the different considered temperatures. The experimental hysteresis cycles shown in Fig. 8 are the same than those shown in Fig. 2 but for the magnetization $M(H)$ instead of the flux density $B(H)$. As can be seen in Fig. 9, the five parameters show a monotonic evolution with temperature. In the model, the parameters actually have a physical interpretation, and it is of interest to investigate how the temperature affects them. The dimensionless parameter c gives the part of anhysteretic magnetization with respect to the irreversible component. The value of c is between 0 and 1 so that if $c = 1$, the material's behavior is purely anhysteretic. The value of c exhibits a monotonic increase from 0.3 to 0.83 between 77 K and 293 K (Fig. 9(a)). The pinning parameter k expressed in A/m gives the coercivity and is directly related to the hysteresis energy losses. In the limit case of very soft ferromagnets, one can assume $k \approx H_c$, where H_c is the coercive field. In the present case, the value of k (Fig. 9(b)) is found to be 1.5-3 times larger than H_c but its value decreases with temperature, a behavior which is consistent with the evolution of H_c observed in Fig. 5. The parameter a, expressed in A/m, is defined as

$$a = \frac{k_B T}{\mu_0 m}, \qquad (17)$$

where k_B is the Boltzmann constant and m is the magnetic moment of a typical magnetic domain. The parameter a (Fig. 9(c)) exhibits a monotonic increase with temperature. The non-linear temperature dependence of a with an upward concavity indicates that the average magnetic moment of magnetic domains decreases with temperature. It is worth mentioning that if we assume that the saturation magnetization is given by $M_s = nm$, the evolution of the density of magnetic domains n is given by
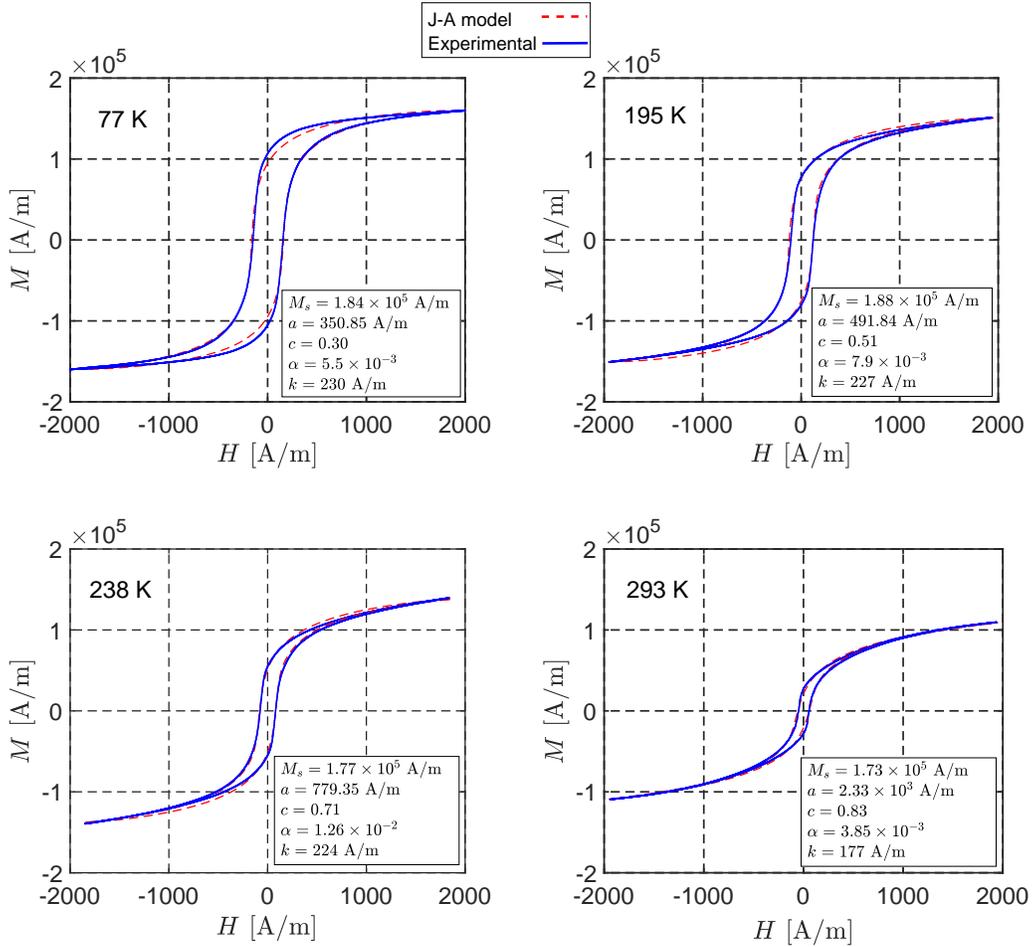
$$n \propto \frac{aM_s}{T}. \qquad (18)$$

Fig. 8. Fitting of the experimental hysteresis cycles (in blue) with the J-A model (in dashed red) at the different investigated temperatures as well as the corresponding fitting parameters.

The dimensionless parameter α (Fig. 9(d)), defining the coupling between magnetic domains, is found to increase with temperature while being much smaller than 1 for all investigated temperatures. Finally, the saturation magnetization M_{s} is plotted in Fig. 9(e). A first estimation of the saturation magnetization is obtained assuming that the magnetization M_{m} at high field follows a law of type

$$M_{\mathrm{m}}(H_{\mathrm{m}}) = M_{\mathrm{s}} - \frac{b}{H_{\mathrm{m}}}. \qquad (19)$$

This M_{s} is then considered as a fifth parameter in the J-A model and the first estimation is adjusted with the other J-A parameters to obtain a good agreement between the model and the experimental results. The saturation magnetization is found to be weakly temperature-dependent. The M_{s} values can be compared to those obtained on Ni-5at.%W using commercial magnetometers. At $T = 300$ K, Gao $et\ al.$ measured M_{s} in the range 11.98-13.04 emu/g (corresponding to $1.25 - 1.45 \times 10^5$ A/m, assuming a density of 9.64 g/cm^3). Song $et\ al.$ determined M_{s} values of ~ 14 G cm^3/g (1.35×10^5 A/m) at 298 K and ~ 25 G cm^3/g (2.4×10^5 A/m) at 77 K. At $T = 5$ K, Ijaduola $et\ al.$ determined M_{s} in the range 27.4-28 (G cm^3/g),

corresponding to $2.64 - 2.69 \times 10^5$ A/m. As a result, the M_{s} value seems to be underestimated at low temperature (77 K) and, on the contrary, overestimated at room temperature compared to previous works. It is likely that this difference originates from the fact that the hysteresis cycles are obtained at a maximum magnetizing field H_{m} which is too low to bring the material close to saturation. In spite of this discrepancy, M_{s} is found to decrease with temperature and the values allow the experimental hysteresis cycles to be reproduced using the J-A model. It can be also noticed that the exact knowledge of the parameter M_{s} does not affect the power law behavior discussed in Section III-E.

IV. Conclusion

In this work, we investigated the magnetic properties of the Ni-5at.%W substrate of coated conductors tapes at several temperatures. The measurements were carried out on a toroidal stack of coated conductors which constitutes naturally a closed magnetic circuit and is the ideal configuration due to the absence of demagnetizing effect. The superconductor contribution to the losses is negligible as the field was applied
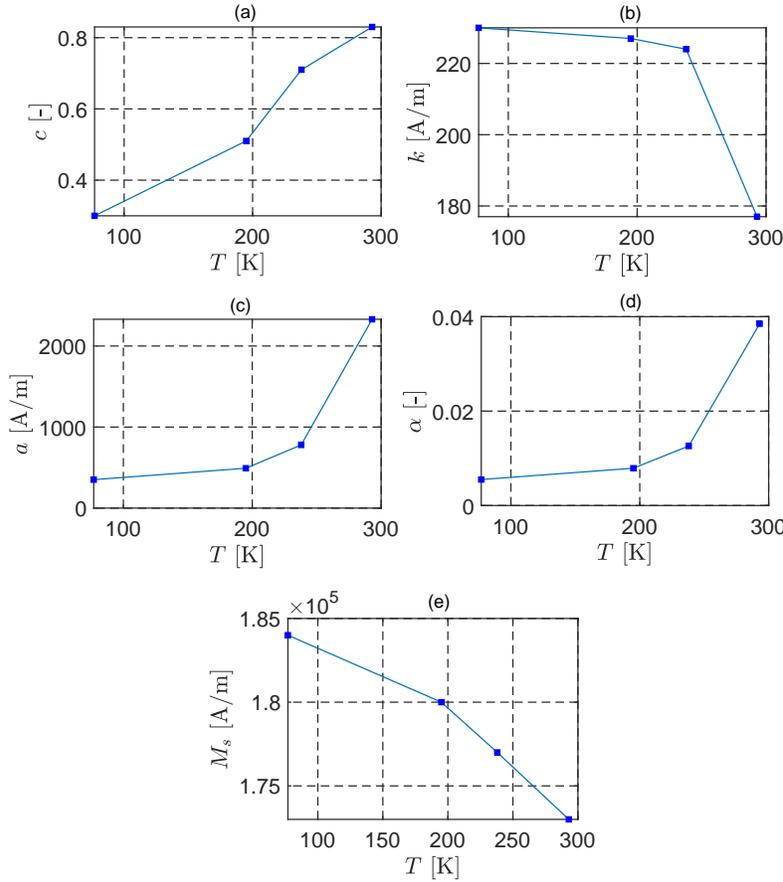
Fig. 9. Evolution of the J-A model parameters as a function of temperature.

were shown to be consistent with the Rayleigh model. Finally, the results were reproduced using the phenomenological Jiles-Atherton model. The five parameters of the model have been identified at different temperatures and exhibit a monotonic evolution. Consequently, these results can be used to obtain, by interpolation, the magnetic properties at every temperatures between 77 K and 293 K and at every magnetic fields below 2000 A/m in order to take into account the magnetic behavior of the Ni-5at.%W substrate when designing systems using RABiTS. Such systems can be found in several applications, including magnetic shielding applications where the ferromagnetic properties of the substrate can be usefully exploited, even above the critical temperature T_c.

ACKNOWLEDGMENTS

REFERENCES

[1] A. Patel, S.C. Hopkins and B.A. Glowacki, "Trapped fields up to 2 T in a 12 mm square stack of commercial superconducting tape using pulsed field magnetization", *Supercond. Sci. Technol.*, vol. 26, Jan. 2013, Art. no. 032001.
[2] L. Wéra, J.F. Fagnard, G.A. Levin, B. Vanderheyden and P. Vanderbemden, "Magnetic shielding with YBCO Coated Conductors: Influence of the Geometry on Its Performances", *IEEE Trans. Appl. Supercond.*, vol. 23, no. 3, June 2013, Art. no. 8200504.
[3] P. Seidel (Ed.), "Applied Superconductivity: Handbook on Devices and Applications", vol. 1, New York: Wiley, 2015.
[4] A. Goyal, M. Parans Paranthaman and U. Schoop, "The RABiTS approach: Using Rolling Assisted Biaxially Textured Substrates for high performance YBCO superconductors", *MRS Bull.*, vol. 29, Aug. 2004, pp. 552-561.
[5] B. de Boer, N. Reger, L. Fernandez G.-R., J. Eickemeyer, B. Holzapfel, L. Schultz, W. Prusseit and P. Berberich, "Biaxially textured Ni-alloy tapes as substrates for buffer and YBCO film growth", *Physica C*, vol. 351, 2001, pp. 38-41.
[6] D.T. Verebelyi *et al.*, "Uniform performance and continuously processed MOD-YBCO-coated conductors using a textured Ni-W substrate", *Supercond. Sci. Technol.*, vol. 16, Mar. 2003, pp. L19-L22.
[7] A. Sanchez, N. Del-Valle, C. Navau and D. Chen, "Influence of magnetic substrate in the transport critical current of superconducting tapes", *Appl. Phys. Lett.*, vol. 97, July 2010, Art. no. 072504.
[8] F. Gömöry, E. Pardo, M. Vojenciak and J. Souc, "Magnetic Flux Penetration and Transport AC Loss in Superconductor Coated Conductor on Ferromagnetic Substrate", *IEEE Trans. Appl. Supercond.*, vol. 19, no. 3, June 2009.
[9] F. Gömöry, M. Vojenciak ,E. Pardo, M. Solovyov and J. Souc, "AC losses in coated conductors", *Supercond. Sci. Technol.*, vol. 23, Feb. 2010, Art. no. 034012.
[10] O. Tsukamoto, H. Nakayama, S. Odaka, M. Ciszek, S. Hahakura, M. Ueyama, K. Ohmatsu and D. Miyagi, "Transport current losses in HoBaCuO-123 coated conductors with a Ni-alloy substrate", *Physica C*, vol. 426-431, 2005, pp. 1290-1294.
[11] D. Miyagi, S. Yamashita, N. Takahashi and O. Tsukamoto, "Study of AC Loss Characteristics of HTS-coated Conductor with Magnetic Substrate Using FEM Analysis", *J. Supercond. Nov. Magn.*, vol. 24, 2011, pp. 43-48.
[12] M. Erdogan, S. Tunc and F. Inanir, "AC Loss Analysis of HTS Pancake Coil of Coated Superconductors with Ferromagnetic Substrate", *J. Supercond. Nov. Magn.*, vol. 30, 2017, pp. 1993-1999.
[13] S. Li, D.-X. Chen and J. Fang, "Transport ac losses of a second-generation HTS tape with a ferromagnetic substrate and conducting stabilizer", *Supercond. Sci. Technol.* vol. 28, Nov. 2015, Art. no. 125011.
[14] G. Liu, G. Zhang, L. Jing, H. Yu, L. Ai, W. Yuan and W. Li, "Influence of Substrate Magnetism on Frequency-Dependent Transport Loss in HTS-Coated Conductors", *IEEE Trans. Appl. Supercond.*, vol. 27, no. 8, Dec. 2017, Art. no. 6603807.

parallel to the tapes. The $B(H)$ hysteresis loops were obtained in AC regime (30 Hz) at 293, 238, 195 and 77 K. No significant effect of frequency was observed in the 20-200 Hz range, showing that the losses are mainly hysteretic in this regime. The results were compared to those already obtained in the literature, at room temperature and liquid nitrogen temperature. The relative permeability was found to exhibit a non monotonic behavior, with a smooth evolution between 293 and 77 K. The $\mu_r(B_m)$ curves show that the temperature does not have a major effect on the peak intensity of the relative permeability. Nevertheless, the maximum permeability at room temperature and liquid nitrogen temperature are different from those found in literature [36]. Moreover, the values of the permeability extrapolated at zero flux density are higher that those reported in previous works, with a difference between room and liquid nitrogen temperatures much less marked than what is reported by Miyagi *et al.* [36]. Interestingly, it was found that the experimental points at 77 K can be fitted with a simple parabolic law between 0 and 0.2 T. The coercive field measured for the high amplitude cycles was found to exhibit a linear decrease with temperature. The hysteresis losses were found to follow a power law at low fields and were expressed as a function of the dimensionless ratio (M/M_s), with and without a DC bias field. The power law exponents

[15] G. Liu, G. Zhang, H. Yu, L. Jing, L. Ai and Q. Liu, "Experimental and numerical study of frequency-dependent transport loss in $YBa_2Cu_3O_{7-\delta}$ coated conductors with ferromagnetic substrate and copper stabilizer", *J. Appl. Phys.*, vol. 121, June 2017, Art. no. 243902.

[16] A. He, C. Xue, H. Yong and Y. Zhou, "Effect of soft ferromagnetic substrate on ac loss in 2G HTS power transmission cables consisting of coated conductors", *Supercond. Sci. Technol.*, vol. 27, 2014 , Art. no. 025004.

[17] X. Li, L. Ren, Y. Xu, J. Shi, X. Chen, G. Chen, Y. Tang and J. Li, "Calculation of CORC Cable Loss Using a Coupled Electromagnetic-Thermal T-A Formulation Model", *IEEE Trans. Appl. Supercond.*, vol. 31, no. 4, June 2021, Art. no. 4802707.

[18] M. Zhang, J. Kvitkovic, J-H. Kim, S.V Pamidi and T.A. Coombs, "Alternating current loss of second-generation high-temperature superconducting coils with magnetic and non-magnetic substrate", *Appl. Phys. Lett.*, vol. 101, Sept. 2012, Art. no. 102602.

[19] M. Niu, H. Yong, J. Xia and Y. Zhou, "The Effects of Ferromagnetic Disks on AC Losses in HTS Pancake Coils with Nonmagnetic and Magnetic Substrates", *J. Supercond. Nov. Magn.*, vol. 32, 2019, pp. 499-510.

[20] Y. Statra, H. Menana and B. Douine, "Integral Modeling of AC Losses in HTS Tapes With Magnetic Substrates", *IEEE Trans. Appl. Supercond.*, vol. 32, no. 2, Mar. 2022, Art. no. 5900407.

[21] A. Musso, M. Breschi, P.L. Ribani and F. Grilli, "Analysis of AC Loss Contributions From Different Layers of HTS Tapes Using the A-V Formulation Model", *IEEE Trans. Appl. Supercond.*, vol. 31, no. 2, Mar 2021, Art no. 5900411.

[22] G.P. Lousberg, J.F. Fagnard, M. Ausloos, P. Vanderbemden and B. Vanderheyden, "Numerical Study of the Shielding Properties of Macroscopic Hybrid Ferromagnetic/Superconductor Hollow Cylinders", *IEEE Trans. Appl. Supercond.*, vol. 20, no. 1, Feb. 2010, pp. 33-41.

[23] J. Kvitkovic, S. Patel and S. Pamidi, "Magnetic Shielding Characteristics of Hybrid High-Temperature Superconductor/Ferromagnetic Material Multilayer Shields", *IEEE Trans. Appl. Supercond.*, vol. 27, no. 4, June 2017, Art. no. 4700705.

[24] L. Gozzelino, R. Gerbaldo, G. Ghigo, F. Laviano, M. Truccato and A. Agostino, "Superconducting and hybrid systems for magnetic field shielding", *Supercond. Sci. Technol.*, vol. 29, Jan. 2016, Art. no. 034004.

[25] A. Bergen, H.J. van Weers, C. Bruineman, M.M.J. Dhallé, H.J.G. Krooshoop, H.J.M. ter Brake, K. Ravensberg, B.D. Jackson and C.K. Wafelbakker, "Design and validation of a large-format transition edge sensor array magnetic shielding system for space application", *Rev. Sci. Instrum.*, vol. 87, Oct. 2016, Art. no. 105109.

[26] M. Fracasso, F. Gömöry, M. Solovyov, R. Gerbaldo, G. Ghigo, F. Laviano, A. Napolitano, D. Torsello and L. Gozzelino, "Modelling and Performance Analysis of MgB_2 and Hybrid Magnetic Shields", *Materials*, vol. 15, 667, Jan. 2022.

[27] P. Vanderbemden, L. Wera, J.F. Fagnard, S. Hahn and An Patel, "Magnetic shielding above 0.7 T at 77 K using a stack of 2G coated conductor tape annuli", Sept. 2019, Presented at the EUCAS 2019 conference (unpublished).

[28] S. Tumanski, "Handbook of Magnetic Measurements", *CRC Press*, Fl, USA, 2011.

[29] D. Miyagi, D. Tome, M. Nakano and N. Takahashi, "Measurement of Magnetic Properties of Nonoriented Electrical Steel Sheet at Liquid Nitrogen Temperature Using Single Sheet Tester", *IEEE Trans. Magn.*, vol. 46, no. 2, Feb. 2010, pp. 314-317.

[30] T. Nakata, Y. Kawase and M. Nakano, "Improvement of measuring accuracy of magnetic field strength in single sheet testers by using two H coils", *IEEE Trans. Magn.*, vol. Mag-23, no. 5, Sept. 1987, pp. 2596-2598.

[31] A.O. Ijaduola, J.R. Thomson, A. Goyal, C.L.H. Thieme and K. Marken, "Magnetism and ferromagnetic loss in Ni–W textured substrates for coated conductors", *Physica C*, vol. 403, 2004, pp. 163-171.

[32] F. Grilli, S.P. Ashworth and L. Civale, "Interaction of magnetic field and magnetic history in high-temperature superconductors", *J. Appl. Phys.*, vol. 102, Oct. 2007, Art. no. 073909.

[33] M. Gao, F. Zhang, S. Liang, H. Li, L. Ma, M. Liu, S. Kausar and H. Suo, "Comparative Characterization of Magnetic Properties of Textured Ni-5 at.%W Alloy Subtstrates", *J. Supercond. Nov. Magn.*, vol. 32, 2019, pp. 1489-1495.

[34] J.H. Claassen and C.L.H. Thieme, "Magnetic properties of Ni-based substrates for HTS tape", *Supercond. Sci. Technol.*, vol. 21, July 2008, Art. no. 105003.

[35] J.H. Claassen, M.A. Willard, T.L. Francavilla and V.G. Harris, "Inductive measurements of magnetic properties of ribbon materials", *Rev. Sci. Instrum.*, vol. 75, no. 9, Sept. 2004, pp. 2817-2821.

[36] D. Miyagi, Y. Yunoki, M. Umabuchi, N. Takahashi and O. Tsukamoto, "Measurement of magnetic properties of Ni-alloy substrate of HTS coated conductor in LN_2", *Physica C*, vol. 468, July 2008, pp. 1743-1746.

[37] D.N. Nguyen, S.P. Ashworth, J. O. Willis, F. Sirois and F. Grilli, "A new finite-element method simulation model for computing AC loss in roll assisted biaxially textured substrate YBCO tapes", *Supercond. Sci. Technol.*, vol. 23, 2010, Art. no. 025001.

[38] D.C. Jiles and D.L. Atherton, "Theory of ferromagnetic hysteresis", *J. Appl. Phys.*, vol. 55, no. 6, 1984, pp. 2115-2120.

[39] S. Hahn, J. Voccio, D.K. Park, K.-M. Kim, M. Tomita, J. Bascuñán and Y. Iwasa, "A Stack of YBCO Annuli, Thin Plate and Bulk, for Micro-NMR Spectroscopy", *IEEE Trans. Appl. Supercond.*, vol. 22, no. 3, June 2012, Art. no. 4302204.

[40] A. Patel, S. Hahn, J. Voccio, A. Baskys, S.C. Hopkins and B.A. Glowacki, "Magnetic levitation using a stack of high temperature superconducting tape annuli", *Supercond. Sci. Technol.*, vol. 30, 2017, Art. no. 024007.

[41] K.J. Song, Y.M. Park, J.S. Yang, S.W. Kim, R.K. Ko, H.S. Kim, H.S. Ha, S.S. Oh, C. Park, J.H. Joo and C.J. Kim, "Magnetism in Ni-W textured substrates for coated conductors", *Journal of the Korea Institute of Applied Superconductivity and Cryogenics*, vol. 7, no. 7, 2005, pp. 7-10.

[42] G. Bertotti, "Hysteresis in magnetism", *Academic Press, San Diego*, CA, USA, 1998.

[43] N. Takahashi, M. Morishita, D. Miyagi and M. Nakano, "Examination of Magnetic Properties of Magnetic Materials at High Temperature Using a Ring Specimen", *IEEE Trans. Magn.*, vol. 46, no. 2, Feb. 2010, pp. 548-551.

[44] V. Lahtinen, E. Pardo, J. Souc, M. Solovyov and A. Stenvall, "Ripple field losses in direct current biased superconductors: Simulation and comparison with measurements", *J. Appl. Phys.*, vol. 115, Mar. 2014, Art. no. 113907.

[45] S. Takahashi and S. Kobayashi, "Scaling power-law relations in asymmetrical minor loops", *J. Appl. Phys.*, vol. 107, Mar. 2010, Art. no. 063903.

[46] S. Kobayashi, S. Takahashi, T. Shishido, Y. Kamada and H. Kikuchi, "Low-field magnetic characterization of ferromagnets using a minor-loop scaling law", *J. Appl. Phys.*, vol. 107, Jan. 2010, Art. no. 023908.

[47] F. Fiorillo, "Measurement and Characterization of Magnetic Materials", *Elsevier*, Amsterdam, 2004.

[48] N.C. Pop and O.F. Caltun, "Jiles–Atherton Magnetic Hysteresis Parameters Identification", *Acta Phys. Pol. A*, vol. 120, no. 3, Feb. 2011, pp. 491-496.

[49] D.C. Jiles and J.B. Thoelke, "Theory of ferromagnetic hysteresis: Determination of model parameters from experimental hysteresis loops", *IEEE Trans. Magn.*, vol. 25, no. 5, Sept. 1989, pp. 3928-3930.